Reaction mechanism coexistence in the 123 MeV $^{19}F+^{56}Fe$ reaction

A. Brondi, M. Kildir,* G. La Rana, R. Moro, and E. Vardaci
Istituto Nazionale di Fisica Nucleare and Dipartimento di Scienze Fisiche dell' Universitá di Napoli, Napoli, Italy

S. Pirrone, F. Porto, S. Sambataro, G. Politi, and P. Figuera
Istituto Nazionale di Fisica Nucleare and Dipartimento di Fisica di Catania and Laboratorio Nazionale del Sud, Catania, Italy

(Received 19 June 1996)

Mass and charge identified ejectiles, spanning from ^{11}B to ^{22}Ne, have been detected in the 123 MeV $^{19}F+^{56}Fe$ reaction. The coexistence of deep inelastic collision (DIC) and incomplete fusion (IF) mechanisms has been observed. The shape of the energy spectra and their behavior with angle allowed us to identify two components: The less dissipative one was dominating near the grazing angle. For both components experimental optimum Q values were derived. Two approaches based on the sum rule (SR) model of Wilczyński were used to calculate DIC and IF contributions to the complex fragment cross sections. Both prescriptions fit reasonably well experimental ejectile cross sections and Q optimum values. Results of the present investigation support the idea that the DIC can be treated on the same footing as IF in the SR model once the first process is confined in an inner angular momentum window, starting from the maximum fusion angular momentum, with respect to quasielastic processes. [S0556-2813(96)05510-0]

PACS number(s): 25.70.Hi, 25.70.Lm

I. INTRODUCTION

The study of complex fragment emission in heavy-ion reactions has been effective in probing the onset and coexistence of different mechanisms such as incomplete fusion (IF) and deep inelastic collisions (DIC's). However, the goal of having a comprehensive description of the mechanisms involved is far from being achieved, especially at relatively low energy (around 5–6 MeV per nucleon) where the cross sections of the two processes are rather small.

It is generally accepted that the IF mechanism originates from the fusion of only part of the projectile with the target. The remnant of the projectile continues its motion with about the beam velocity. Since the pioneer works of Wilczyński and co-workers [1,2] who observed the IF mechanism in reactions between very asymmetric heavy-ion partners at energies around 10 MeV per nucleon, a number of experiments have observed IF events in a wide range of masses and energies of incoming ions [3–5]. In particular, for medium-light systems several investigations studied the IF process mainly with the aim of studying the onset of the IF mechanism [6–8]. Morgenstern *et al.* [9] related the appearance of this process to the relative velocity of the incident ions.

On the other hand, the DIC process, characterized by the dissipation of a significant amount of the incident kinetic energy and angular momentum into excitation energy and intrinsic spin of the products, have focused much attention [10]. This mechanism has been mainly studied in heavy systems but, although appearing with different features, its occurrence in medium-light systems has been definetively recognized [10].

More recently, the coexistence of IF and DIC mechanisms has been observed in the $^{30}Si+^{30}Si$ [11] and $^{19}F+^{64}Ni$ [12] reactions at low bombarding energy. The DIC and IF mechanisms were predominant in the first and second reactions, respectively. In the $^{30}Si+^{30}Si$ system IF is responsible for large massive transfers while DIC dominates in the emission of quasiprojectiles. A different behavior was found for the asymmetric system $^{19}F+^{64}Ni$ where measured Q value spectra show the dominance of the incomplete fusion mechanism in small massive transfers, while DIC increases with the charge transfer.

From the theoretical point of view, the IF mechanism has been successfully described in many cases by the sum rule

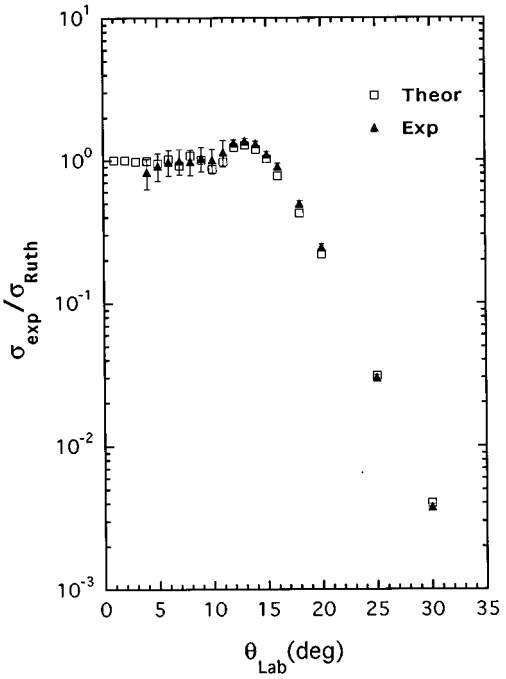

FIG. 1. $^{19}F+^{56}Fe$ elastic scattering angular distribution. The line represents the fit to the data.

*Permanent address: Middle East Technical University, Ankara, Turkey.

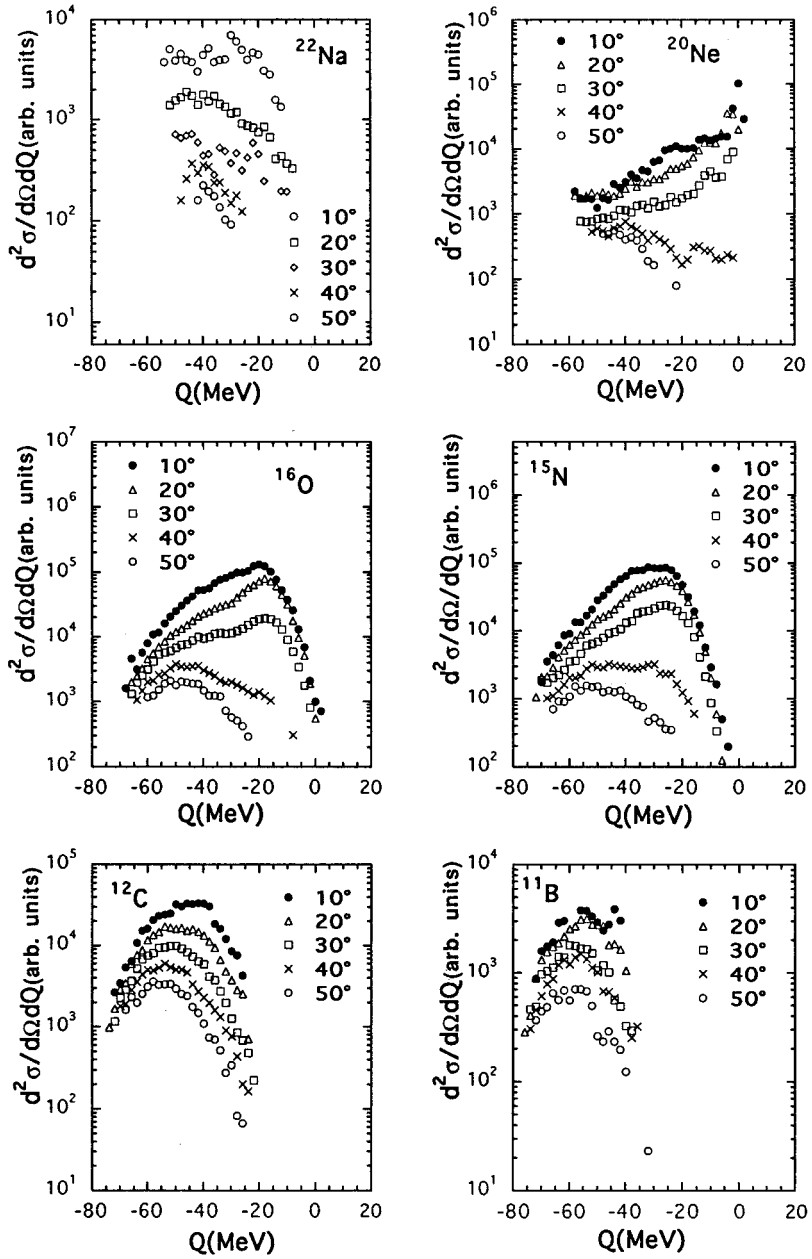

FIG. 2. Center-of-mass energy spectra for the six most populated ejectiles in the reaction ^{19}F+^{56}Fe.

(SR) model [13,14] which is capable of calculating optimum Q values ($Q_{\rm opt}$) and absolute cross sections for each exit channel. The main features of the SR model are the following.

(a) IF channels are localized in narrow windows in the l region above the critical angular momentum for complete fusion ($l_{\rm fus}$), due to the l limitation for each massive transfer.

(b) The relative probabilities of different channels are ruled by the phase space term derived under the assumption of partial statistical equilibrium [15].

Recently, a generalization of the SR model has been developed to account for the DIC mechanism in the same context as IF [12]. In particular, DIC competition is derived introducing in the phase space term Q values calculated for each l in the sticking limit and by limiting the DIC contribution to the $l_{\rm fus}-l_{\rm DIC}$ window. This model, which we will refer to as the DIC incomplete fusion sum rule (DISR1) model, has been applied to the reaction ^{19}F+^{64}Ni at 120 MeV of incident energy. The DIC events were recognized by the measured $Q_{\rm opt}$ values for the most dissipative component in the energy spectra and by the angular distributions for different mass transfers. In this reaction the IF mechanism was predominant, and therefore the inclusion of the DIC in the model slightly improved the agreement in the cross sections.

The Wilczyński model has been also generalized, in a similar way, to account for intermediate mass fragment emission from rather asymmetric systems at energies of tens of MeV per nucleon [16]. The good agreement in reproducing the charge distributions of the fragments supports the validity, also at these energies, of the general assumptions from which the SR model stems.

The present paper reports a further study on the coexistence of DIC and IF mechanisms in a medium mass system at about 6 MeV per nucleon of incident energy. We have studied the system ^{19}F + ^{56}Fe at 123 MeV bombarding energy

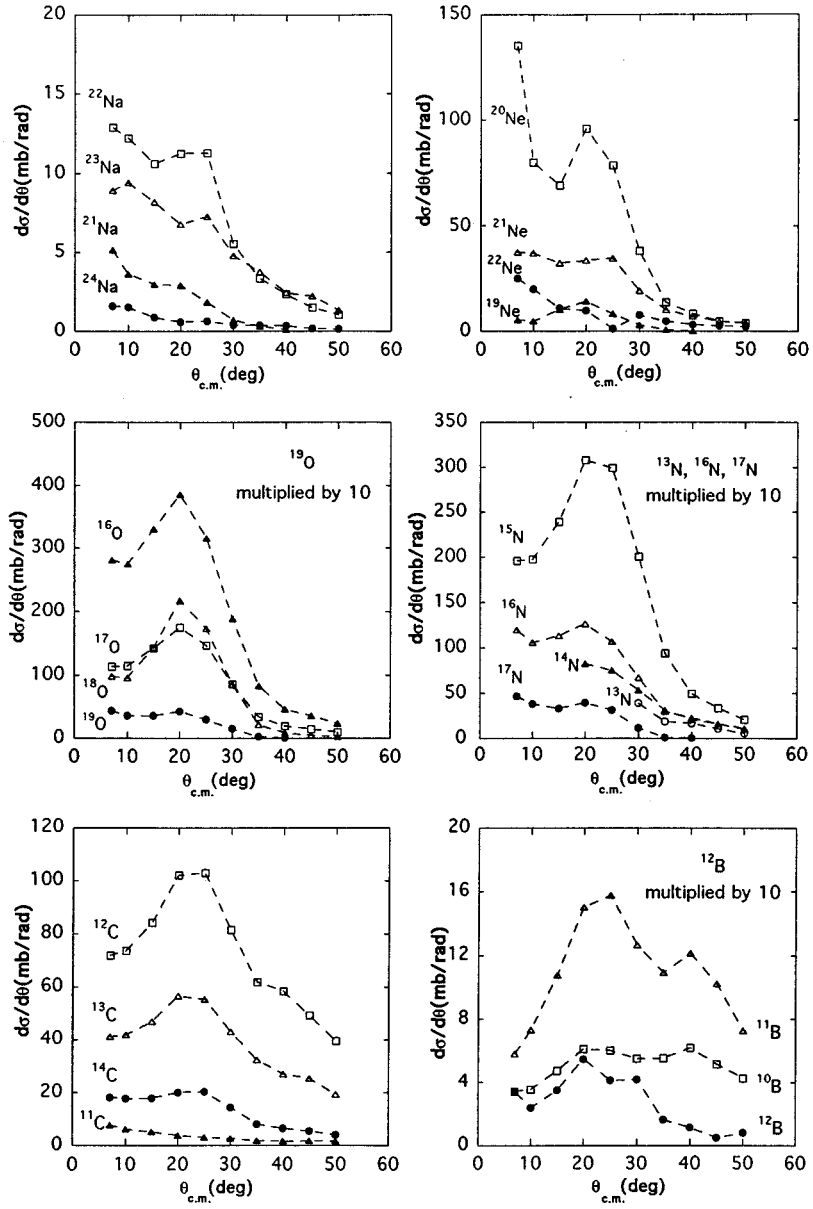

FIG. 3. Ejectile angular distributions in the reaction $^{19}F+^{56}Fe$.

measuring energy spectra and angular distributions of mass and charge identified ejectiles. In order to better test the validity of the SR model as a framework for the description of IF and DIC mehanisms, low thresholds in the energy spectra, measured in a wide range of angles including small forward angles below θ_{graz}, were required, together with a good mass and charge identification. The choice of the system was also motivated by the possibility of using the same values, for the parameters involved in the DISR1 model calculations, as for the system $^{19}F+^{64}Ni$.

II. EXPERIMENTAL PROCEDURE AND DATA ANALYSIS

The experiment was performed at the SMP 13 Tandem of the Laboratorio Nazionale del Sud at Catania. A beam of ^{19}F (8^+ charge state) with laboratory energy of 123 MeV was used to bombard a selfsupporting target of ^{56}Fe (460 $\mu g/cm^2$ thick and 99.7% enriched). Beam currents up to 90 nA were used.

Charge and mass identification, and energy spectra of the ejectiles were obtained using the detection system described in Ref. [17]. This system combines the good energy resolution of a large ionization chamber with the good timing properties provided by microchannel plates and parallel-plate avalanche counters. The latter supplied the start and stop signals of the time of flight, respectively.

This detector assembly was connected to a sliding seal scattering chamber, allowing the rotation from $-20°$ to $+100°$ with respect to the beam direction. The position was electronically controlled with a sensitivity of $6'$. A tantalum collimator (3.2 mm in diameter), placed between the scattering chamber and the detector system, defined a detector solid angle of 0.16 msr.

Two silicon detectors (300 μm thick), to be used as monitors, were placed inside the chamber, at 13° and 17° on opposite sides of the beam. In addition, a small Faraday cup was mounted to control the beam current.

The ionization chamber was divided in two sections, 13 cm and 69 cm long, respectively. Two anode plates provided

TABLE I. Experimental and calculated ejectile Q_{opt} values (MeV) for IF and DIC components. Calculations have been performed using the DISR1 prescription of the model.

Ejectile	Q_{opt}(IF) Expt.	Q_{opt}(IF) Calc.	Q_{opt}(DIC) Expt.	Q_{opt}(DIC) Calc.
^{11}B		−52	−58	−63
^{11}C	−46	−47	−56	−57
^{12}C	−42	−45	−56	−58
^{13}C	−38	−42	−56	−59
^{14}C	−30	−40	−50	−60
^{13}N	−36	−38	−54	−54
^{14}N	−30	−35	−52	−55
^{15}N	−26	−32	−52	−56
^{16}N	−26	−28	−52	−57
^{17}N	−20	−26		−58
^{15}O	−28	−26	−52	−52
^{16}O	−16	−21	−48	−52
^{17}O	−18	−17	−50	−53
^{18}O	−14	−13	−48	−54
^{21}Ne		−11	−40	−49
^{22}Ne	−18	−14	−42	−50

signals proportional to the energy lost in the first and the second sections, respectively. The chamber was operated with P10 gas mixture at the pressure of 260 Torr. The reduced field across cathode and Frisch grid was chosen to be 0.25 V/cm Torr.

The micro-channel-plate detector, manufactured in the Chevron arrangement, provided the start signal for the time of flight measurement. It used a thin carbon foil, 5μg/cm^2 thick, and was mounted at 45° with respect to the detection direction.

The parallel-plate-avalanche counter was operated with isobutane gas at the pressure of 5 Torr and a reduced electric field E/P = 600 V/cm Torr. It was placed 118 cm far away from the micro-channel-plate detector. With this flight distance, the time resolution of 400 ps, measured on the elastically scattered ions, determined a 2% mass resolution.

Energy calibration of the ionization chamber was accomplished by detecting elastically scattered ^{19}F ions from gold (150 μg/cm^2 thick) and Fe targets at different bombarding energies. An energy calibration for each ejectile has been deduced, correcting the measured energy for the energy lost in the target and in the dead layers of the detector system.

TABLE II. Percentages of DIC component in the ejectile cross sections.

Ejectile	Expt.	DISR1	DISR2
^{12}C	70%	25%	59%
^{15}N	17%	8%	12%
^{16}O	13%	3%	4%

To determine the absolute reaction cross section, elastic scattering measurements on ^{56}Fe were performed from 4° to 20° in 1° steps, and at 25° and 30°. Assuming pure Rutherford scattering between 6° and 10°, a conversion factor to determine cross sections from the measured yields was deduced. Normalization between angles was made using the elastic scattering yield measured by the two monitors.

The ratio between the two monitor counting rates changed up to 30% during the measurements, while the statistical uncertainties in the single measurements were always less than 1%. Therefore, we believe that the main source of experimental uncertainty in the counting rates was caused by the variation in the beam localization on the target. Because of the presence of a diaphragm at the entrance of the scattering chamber, a maximum displacement of the beam on the target of about ±2 mm was estimated. The resulting variation in the angular position of the detection system determined an uncertainty in the experimental counting rate for pure Coulomb scattering of about 20% for the forward angles and less than 5% for angles larger than 12°.

Complex fragments were detected in two angular ranges from 4° to 20° and from 25° to 40° in 4° and 5° steps, respectively. Ejectile energies were converted, event by event, to the center-of-mass system, assuming binary kinematics.

III. EXPERIMENTAL RESULTS

The elastic scattering angular distribution is given in Fig. 1. Data were fitted by optical model calculations, using the

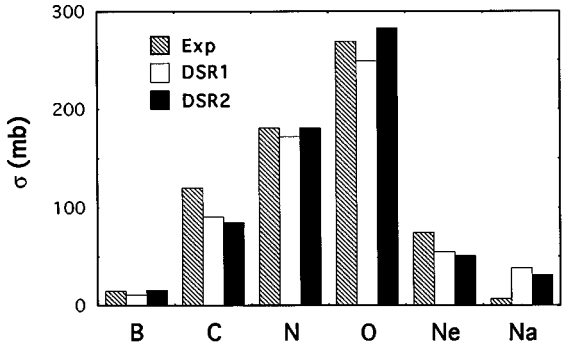

FIG. 4. Elemental cross sections in the reaction ^{19}F+^{56}Fe. Experimental values are compared with those calculated with DISR1 and DISR2 prescriptions.

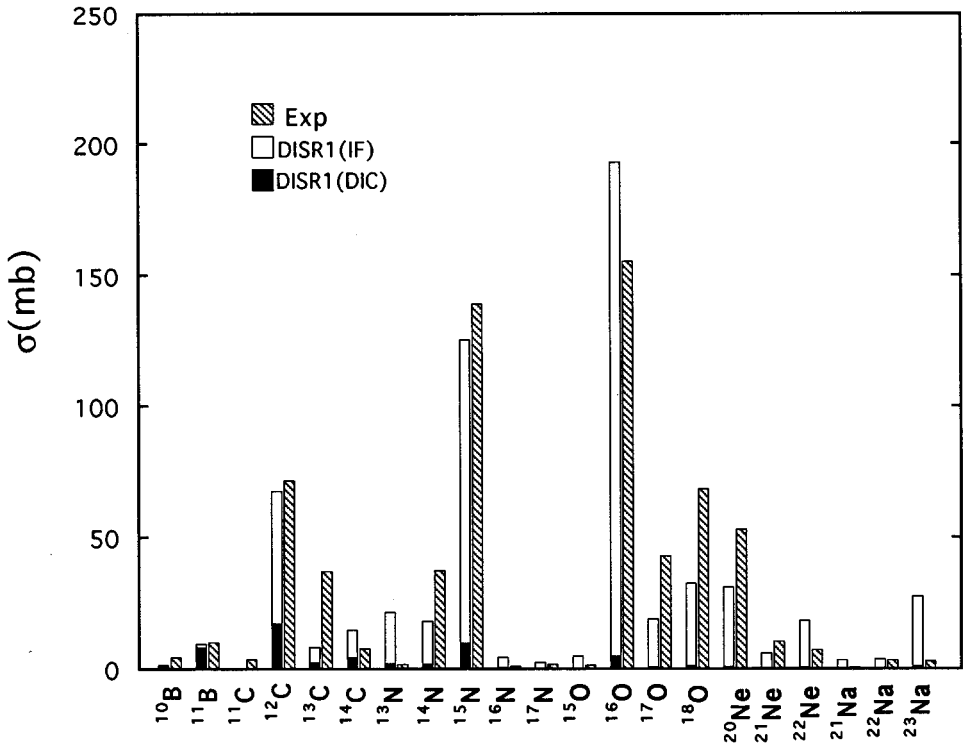

FIG. 5. Experimental cross sections (for $Q \geq Q_{ev}$) for the ejectiles detected in the reaction $^{19}F + ^{56}Fe$ compared to the corresponding cross sections calculated in the DISR1 prescription. White and black bars identify IF and DIC contributions.

code PTOLEMY [18] with potential well depth and diffuseness of 64.10 MeV and 0.4 fm, and 6.65 MeV and 0.5 fm, for the real and imaginary parts, respectively, and $R_0 = 1.3$ fm for the radius of both potentials. The calculated values well agree with experimental points within errors. A reaction cross section of 1937 mb was deduced, which corresponds, in the sharp cutoff approximation, to an $l_{graz} = 63\hbar$.

Ejectiles with Z between 5 and 11 were observed by identifying all the corresponding isotopes except for fluorine ions, owing to the intense elastic scattering yield. Absolute differential cross sections for each channel were deduced, normalizing the counting rate to the corresponding elastic rate.

The shapes of the center-of-mass (c.m.) channel-energy spectra show an evolution with angle more or less rapid depending on the ejectile. In Fig. 2 the energy spectra at different c.m. angles are presented for six isotopes, the most populated one for each element. In Fig. 3 the angular distributions of all the observed ejectiles except for fluorine isotopes are shown. Two components are clearly present in the spectra. The less dissipative component is dominating at forward angles, near the grazing angle ($\theta_{c.m.} = 25°$). In addition, angular distributions vary from ejectile to ejectile, being strongly peaked around the grazing angle for few nucleon transfers and relatively flat for the most massive transfers.

This behavior was already observed for 100 MeV $^{16}O + ^{64}Ni$ [3] and for 120 MeV $^{19}F + ^{64}Ni$ [12] and interpreted as the coexistence of two mechanisms. As in Ref. [12] we will refer the more damped component to DIC and the other component to IF processes. For each identified ejectile two optimum Q values, corresponding to the maxima in the energy spectra at forward and backward angles, have been deduced and are referred to as Q_{opt}(IF) and Q_{opt}(DIC) in Table I.

To obtain the reaction cross section for each eiectile a linear extrapolation was applied to backward angles. The value of the cross section at 0° was estimated as the average between the most forward experimental value and the 0° value obtained by linear extrapolation of the data at the two most forward angles. This choice, to a certain extent arbitrary, was motivated by the physical aspect that orbiting increases cross sections around 0°. The increase in the total ejectile cross section resulting from extrapolation was only 20%.

In order to estimate the contributions of the detected eiectiles which could result from particle emission from the primary ejectiles, we assumed an energy sharing corresponding to equal temperature for the dinuclear system. This assumption is supported by the findings of Ref. [20] for the most dissipative events. For each ejectile we evaluated the Q value corresponding to the nucleon separation energy plus the Coulomb barrier in the case of protons (Q_{ev}). Disregarding the events relative to Q values greater than Q_{ev} we obtained a reduction in the total ejectile cross section of 15%.

Finally, in some favorable cases, we were able to extract the percentage of DIC processes in the ejectile cross section. To this end, we assumed IF events concentrated around the grazing angle and DIC events as having a flat angular distribution deduced from data at $\theta = 60°$. Rough estimates of the percentages of DIC component in the ejectile cross sections were obtained for ^{12}C, ^{15}N, and ^{16}O (Table II).

IV. DISCUSSION

As shown in the preceding section, ejectile energy spectra and angular distributions indicate the presence of two components in the reaction mechanism responsible for the complex ion emission. Apart from these indications calculations assuming only the IF mechanism, using the Wilczyński sum

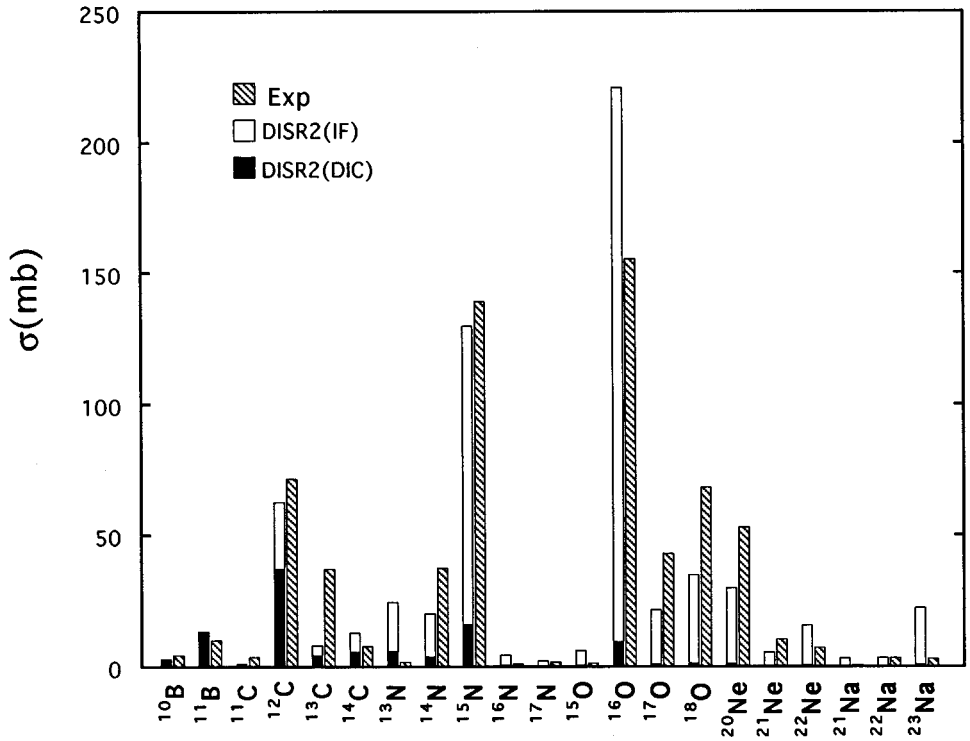

FIG. 6. Experimental cross sections (for $Q \geqslant Q_{ev}$) for the ejectiles detected in the reaction $^{19}F + ^{56}Fe$ compared to the corresponding cross sections calculated in the DISR2 prescription. White and black bars identify IF and DIC contributions.

rule model [13], do not reproduce experimental cross sections, in particular overestimate the ^{12}C production by a factor of 2. Therefore, the theoretical description of Ref. [12] which includes the DIC mechanism in the sum rule model [13,14], was applied. In this approach the cross section for each angular momentum l and channel i is given by

$$\sigma_l(i) = \sigma_l^{\mathrm{IF}}(i) + \sigma_l^{\mathrm{DIC}}(i).$$

The total i channel cross section is then given by

$$\sigma(i) = \pi \lambda^2 \sum_{l=l_{\mathrm{fus}}}^{l_{\mathrm{graz}}} (2l+1) \frac{T_l^{\mathrm{IF}}(i) p_l^{\mathrm{IF}}(i) + T_l^{\mathrm{DIC}}(i) p_l^{\mathrm{DIC}}(i)}{\Sigma_j [T_l^{\mathrm{IF}}(j) p_l^{\mathrm{IF}}(j) + T_l^{\mathrm{DIC}}(j) p_l^{\mathrm{DIC}}(j)]},$$

with

$$p_l^{\mathrm{IF}}(i) = \exp \frac{Q_{gg}(i) - Q_{\mathrm{rad}}^{\mathrm{IF}}(i,l)}{\mathrm{TIF}}$$

and

$$p_l^{\mathrm{DIC}}(i) = \exp \frac{Q_{gg}(i) - Q^{\mathrm{DIC}}(i,l)}{\mathrm{TDIC}}.$$

The quantities p_l^{IF}(i) and p_l^{DIC}(i) represent the probability factors. The Q_{rad} is given by the Coulomb energy difference between the entrance and exit channels, ΔQ_C, plus the radial kinetic energy dissipated at the interaction radius [12]. The Q_{DIC} is calculated in the sticking limit as in Ref. [11]. The TIF and TDIC are temperature parameters.

The transmission coefficients for IF and DIC mechanisms were given by

$$T_l^{\mathrm{IF}}(i) = \left(1 + \exp \frac{l - l_{\mathrm{lim}}(i)}{a_{\mathrm{IF}}}\right)^{-1}$$

and

$$T_l^{\mathrm{DIC}} = \left(1 + \exp \frac{l - l_{\mathrm{DIC}}}{a_{\mathrm{DIC}}}\right)^{-1},$$

respectively.

The l_{lim}(i) is the entrance channel maximum angular momentum for the i channel defined by Wilczyński and l_{DIC} is a limiting angular momentum for DIC independent of the channel; a_{IF} and a_{DIC} are the diffuseness in the l space for IF and DIC, respectively.

Calculations have been performed with this prescription (DISR1) retaining the values of the temperatures and diffuseness in l space for IF and DIC of Ref. [12], that is, TIF = 3 MeV, TDIC = 3.5 MeV, and $a = 0.5\hbar$ for both mechanisms. The maximum angular momentum for fusion, $l_{\mathrm{fus}} = 39\hbar$, was derived by the Krappe-Nix-Sierk potential [19]. The l_{graz} of $63\hbar$ deduced by the measured elastic scattering was used. The best fit to the experimental elemental cross sections shown in Fig. 4 gave an $l_{\mathrm{DIC}} = 49\hbar$.

Calculated optimum Q values for DIC and IF mechanisms were then obtained by weighting the l dependent Q values with the corresponding cross sections, and are reported in Table I. In this calculation, the Q values for IF were obtained using the l dependent optimum Q value formula of Ref. [14].

Calculated ejectile cross sections are compared to the experimental values deduced for Q values greater than Q_{ev} in Fig. 5. The contributions of DIC and IF processes to the calculated cross sections are indicated as white and black bars for IF and DIC, respectively. The calculated percentage of DIC summed over all the observed ejectiles is about 10%.

The DIC process results to be dominant in the $l_{\mathrm{fus}} - l_{\mathrm{DIC}}$ window because of the larger Q_{DIC} values while most of the

cross section IF process is confined in the $l_{\mathrm{DIC}}-l_{\mathrm{graz}}$ window. The agreement between calculated and experimental ejectile cross sections and Q_{opt} values is reasonably good.

Calculated DIC percentages for ^{12}C, ^{15}N, and ^{16}O ejectiles are compared to the experimental ones in Table II. The DIC percentages appear underestimated by the calculation. Attempts to reproduce them increasing l_{DIC} essentially produces an increase in the DIC cross sections for ejectiles lighter than boron, worsening the agreement in the cross sections for all the observed ejectiles. In order to better reproduce the DIC percentages, calculations have been performed using a different approach of including DIC in the SR model (DISR2). It consists in adopting the original sum rule phase-space term governed by the $Q_{gg}-\Delta Q_C$ for both IF and DIC processes [13].

Model parameters were established by the best agreement on the elemental cross sections and resulted to be the same as for DISR1, except for the l_{DIC} which is 51 with respect to 49 in the DISR1 calculation.

Calculated cross sections for each element are similar for both prescriptions and compare well with experimental data (see Fig. 4).

In Fig. 6 the DISR2 calculated cross sections for each ejectile are shown and compared to the experimental cross sections for $Q \geqslant Q_{\mathrm{ev}}$. White and black bars identify the IF and DIC contributions. The calculated Q_{opt} values are essentially the same than those obtained with DISR1 prescription. The calculated DIC percentages for ^{12}C, ^{15}N, and ^{16}O ejectiles are reported in Table II. While for the cross sections comparable agreement is achieved, the calculated DIC percentages are quite different in the case of ^{12}C. A better agreement with experimental values is achieved in the second approach. To draw conclusions from all these results we have to make some remarks. The two approaches we have followed are very similar because they both rely on the sum rule model and include IF and DIC mechanisms.

Both prescriptions were capable of fitting data using as free parameter only the l_{DIC}. All this gives support to the idea that the leading parameter to describe IF and DIC mechanisms is the angular momentum. More precisely, the confinement of the DIC process in an inner l window with respect to the IF process appears to be essential to produce good agreement with data. In fact, calculations carried out disregarding this constraint, in both prescriptions, were unable to reproduce Q values and ejectile cross sections. This conclusion also fits in the general picture in which dissipative processes correspond to smaller impact parameters and involve longer interaction times with respect to quasielastic processes.

ACKNOWLEDGMENTS

The authors wish to acknowledge the cooperation of the Tandem operating staff of Laboratorio Nazionale del Sud at Catania.

[1] K. Siwek-Wilczyńska, E. H. du Marchie van Voorthuysen, J. van Popta, R. H. Siemssen, and J. Wilczyński, Phys. Rev. Lett. **42**, 1599 (1979).

[2] J. Wilczyński, K. Siwek-Wilczyńska, J. van Driel, S. Gonggrijp, D. C. J. M. Hageman, R. V. F. Janssens, J. Lukasiak, and R. H. Siemssen, Phys. Rev. Lett. **45**, 606 (1980).

[3] A. Brondi, G. Cavaccini, A. D' Onofrio, G. La Rana, R. Moro, V. Roca, M. Romano, G. Spadaccini, F. Terrasi, and M. Vigilante, Nucl. Phys. **A489**, 547 (1988).

[4] E. A. Bakkum, P. Decowski, K. A. Griffioen, R. J. Meijer, and R. Kamermans, Nucl. Phys. **A511**, 117 (1990).

[5] B. S. Tomar, A. Goswami, A. V. R. Reddy, S. K. Das, P. P. Burte, S. B. Manohar, and J. Bency, Phys. Rev. C **49**, 941 (1994) and references therein.

[6] G. Rosner, J. Pochodzalla, B. Hech, G. Hlawatsch, A. Miczaika, H. J. Rabe, R. Butsch, B. Kolb, and B. Sedelmeyer, Phys. Lett. **150B**, 87 (1985).

[7] H. Ikezoe, N. Shikazono, Y. Tomita, K. Ideno, Y. Sugiyama, and E. Takekoshi, Nucl. Phys. **A444**, 349 (1985).

[8] D. J. Parker, J. Asher, T. W. Conlon, and I. Naqib, Phys. Rev. C **30**, 143 (1984).

[9] H. Morgenstern, W. Bohne, W. Galster, and K. Grabisch, Z. Phys. A **324**, 443 (1986).

[10] W. U. Schröder, and J. R. Huizenga, in *Treatise on Heavy-Ion Science*, edited by D. A. Bromley (Plenum, New York, 1985), Vol. 2, p. 115.

[11] R. Moro, G. La Rana, A. Brondi, P. Cuzzocrea, A. D'Onofrio, E. Perillo, M. Romano, F. Terrasi, E. Vardaci, and H. Dumont Nucl. Phys. **A477**, 120 (1988).

[12] F. Terrasi, A. Brondi, G. La Rana, G. De Angelis, A. D'Onofrio, R. Moro, E. Perillo, and M. Romano, Phys. Rev. C **40**, 742 (1989).

[13] J. Wilczyński, K. Siwek-Wilczyńska, J. van Driel, S. Gonggrijp, D. C. J. M. Hageman, R. V. F. Janssens, J. Lukasiak, R. H. Siemssen, and S. Y. Van der Werf, Nucl. Phys. **A373**, 109 (1982).

[14] J. Wilczynski, in *Proceedings of the International Conference on Nuclear Physics*, Florence, 1983, edited by R. A. Ricci and P. Blasi (Tipografia Compositori, Bologna, 1983), p. 305.

[15] J. P. Bondorf, F. Dickmann, D. H. E. Gross, and P. J. Siemens, J. Phys. (Paris) Colloq. **32**, C6-145 (1971).

[16] I. M. Brâncuş, H. Rebel, J. Wentz, and V. Corcalciuc, Phys. Rev. C **42**, 2157 (1990).

[17] P. Figuera, S. Pirrone, A. Anzalone, N. Arena, SB. Cavallaro, S. Feminó, F. Giustolisi, F. Porto, and S. Sambataro, Nuovo Cimento A **104**, 251 (1991).

[18] M. H. Macfarlane, and S. C. Pieper, Argonne National Laboratory Report No. ANL-76-11, 1978.

[19] H. J. Krappe, J. R. Nix, and A. J. Sierk, Phys. Rev. C **20**, 992 (1979).

[20] A. Brondi, G. de Angelis, A. D'Onofrio, G. La Rana, R. Moro, V. Roca, G. Spadaccini, F. Terrasi , M. Vigilante, R. Alba, G. Bellia, A. Del Zoppo, G. Russo, P. Sapienza, and J. Gomez del Campo, Nucl. Phys. **A552**, 113 (1993).